https://doi.org/10.5194/egusphere-2025-321
Preprint. Discussion started: 3 February 2025
© Author(s) 2025. CC BY 4.0 License.

Modeling wave-vegetation interactions: the impact of seagrass flexibility and seasonal variability

Seimur Shirinov [a,c], Ivan Federico [a], Simone Bonamano [b], Salvatore Causio [a], Nicolás Biocca [a], Viviana Piermattei [a], Daniele Piazzolla [a], Jacopo Alessandri [c], Lorenzo Mentaschi [c], Giovanni Coppini [a], Marco Marcelli [b], and Nadia Pinardi [c]

[a]CMCC Foundation - Euro-Mediterranean Center on Climate Change,Italy
[b]Laboratory of Experimental Oceanology and Marine Ecology, DEB, Tuscia University, Molo Vespucci, Port of Civitavecchia, 00053, Civitavecchia, RM, Italy
[c]Department of Physics and Astronomy, University of Bologna, viale Berti Pichat 6/2, Bologna (BO), Italy

Correspondence: Seimur Shirinov (seimur.shirinov@cmcc.it)

Abstract. This study delves into the intricate dynamics between wave activity and marine vegetation, focusing on *Posidonia oceanica* meadows in the Mediterranean Sea along the Civitavecchia coastal zone (north-eastern Tyrrhenian Sea, Italy). Traditional modeling approaches often oversimplify wave-vegetation interactions and overlook the necessity for robust in-situ observational systems, which can lead to inadequate representations of the dynamic environments where seagrasses thrive. The Digital Twin modelling framework presents a compelling solution, offering comprehensive insights that enhance decision-making for coastal management. We advance wave-vegetation modeling by integrating a refined seagrass representation that encompasses flexibility, seasonal growth dynamics, and phenotypic traits, all informed by site-specific measurements. Applying this model to the Civitavecchia coast demonstrated that integrating observed seasonal variability into the numerical model was crucial for obtaining realistic results. This revealed a mean monthly wave damping capacity variation of up to 10%, intricately driven by seasonal growth dynamics. Spatial assessments unveiled wave height reductions ranging from 10% to 40%, with an average attenuation of 18% across Sites of Community Importance and 24% for seagrass traits over rocky substrate. These findings offer valuable insights into the role of seagrasses as nature-based solution, facilitating more effective coastal management strategies and guiding restoration efforts in vulnerable marine ecosystems.

1 Introduction

It is widely acknowledged that the presence of vegetation patches serves to mitigate wave activity. This phenomenon is observed across various marine habitats, including seagrass fields (Infantes et al. (2012), Paul M. (2012), Sánchez-González et al. (2011)) wetlands (Feagin et al. (2011)), and seaweed communities (Dubi and Tørum (1994), Løvås and Tørum (2001)). Wave-vegetation interactions result in the dissipation of wave energy through mechanical work on plant stems, determined by seagrass traits such as shoot density, canopy height, stiffness, and bending, as well as wave characteristics. This phenomenon, termed wave damping by Dalrymple et al. (1984), effectively diminishes wave heights. Concurrently, this interaction induces an increase in

https://doi.org/10.5194/egusphere-2025-321
Preprint. Discussion started: 3 February 2025
© Author(s) 2025. CC BY 4.0 License.

wavelength, thereby reducing wave steepness. As a result, the presence of vegetation contributes to a localized reduction in sea surface elevation behind the patch (Beudin et al. (2017)).

Numerous numerical studies have investigated wave attenuation by submerged coastal vegetation, with early models frequently simplifying flexible plants as rigid cylinders with varying drag coefficients. Mendez and Losada (2004) formulated an empirical model incorporating wave damping and breaking across vegetation fields of various depths. Suzuki and Dijkstra (2007) employed a volume of fluid (VOF) model to simulate wave attenuation over different beds and vegetation fields, underlining the necessity for further validation concerning the intricate interplay between storm waves and seagrass-induced wave attenuation. Recently, Pillai et al. (2022) evaluated the role of seagrass as a nature-based solution (NBS) by incorporating the wave damping sink term induced by vegetation into the wave action density spectrum equation within the WW3 model, following the approach of Beudin et al. (2017). This development was tested in a coastal region of the Northern Adriatic Sea, where the study identified limitations associated with modeling seagrass as rigid stems, resulting in excessive wave damping. The authors hypothesized that accounting for plant flexibility would yield more realistic outcomes, and a reduced damping capacity compared to rigid formulation. Similarly, Abdolali et al. (2022), through the implementation of the vegetation term in WW3, concluded that excluding the vegetation sink term in marsh environments leads to significant discrepancies between model outputs and observations. Jacob et al. (2023) reached analogous conclusions regarding the application of the SCHISM-WWM modeling framework in conjunction with a rigid vegetation module for the coastal waters of the German Wadden Sea. Luhar and Nepf (2011) sought to develop a physics-based model to predict wave decay in a submerged meadow, accounting for the adaptive responses of flexible plants to wave orbital velocity.

To investigate how flexibility can enhance model performance and, consequently, increase the model's ability to replicate the behavior of seagrass meadows in wave attenuation, specific in-situ measurements within submerged vegetation are essential. The lack of detailed observational data on vegetation characteristics, such as morphology and mechanical properties, poses a challenge (Luhar and Nepf (2016)). Instead, existing models often rely on generalized literature data, which may not fully capture the nuances of different plant species. Moreover, these models tend to overlook seasonal variations in vegetation properties, despite growing evidence of their importance in coastal processes (Jacob et al. (2023)). So far, wave attenuation by seagrass canopies has been primarily measured during experiments in flumes using plant-like covers and in shallow systems where they occupy a large fraction of the water column (Fonseca and Cahalan (1992), Koch and Beer (1996), Mork (1996), Chen et al. (2007), Bradley and Houser (2009)). Limited field measurements have been conducted in meadows that occupy a small fraction of the water column due to challenges in deploying and maintaining instruments and platforms in underwater environments that can withstand intense weather events (Infantes et al. (2012)).

In this study, we aim to integrate numerical simulations with an observational system design, emphasizing the critical importance of continuous data collection and the cohesive application of empirical measurements within numerical models. This holistic approach not only enhances the precision of the simulations but also represents a pivotal aspect of the coastal Digital Twin methodologies, necessitating interaction between real-world data and numerical models (Jeong and Lee (2023)). Ultimately, such synergy seeks to facilitate informed decision-making in dynamic marine environments, supporting forecasts of

https://doi.org/10.5194/egusphere-2025-321
Preprint. Discussion started: 3 February 2025
© Author(s) 2025. CC BY 4.0 License.

environmental extremes to aid in risk assessment and management, while also advancing our understanding of the resilience of NBS systems.

The seagrass species considered in this work is *Posidonia oceanica* (*PO*) that stands out as the most common seagrass species in the Mediterranean Sea, typically found in shallow sub-tidal waters up to a depth of 50 meters under clear conditions (Borum et al. (2004)). Submerged plants increase bottom roughness, reducing near-bed velocities and altering sediment transport (Madsen et al. (2001)), while also enhancing wave attenuation (Mendez and Losada (2004)). On a long timescale the numerical simulations of waves over marine seagrasses have so far been conducted using vegetation parameters that remain constant in space and time (Pillai et al. (2022)). Given that *PO* meadows along the coastal areas exhibit varying characteristics depending on the type of substrate they inhabit (e.g. rock, sand, and degraded matte), it is necessary to consider the spatial and temporal variability of vegetation parameters (shoot density and leaf length) to accurately estimate the wave damping effect. *PO* meadows grow on an inter-annual scale by branching rhizomes horizontally to colonize vacant substrates when environmental conditions are favorable, and vertically to prevent siltation. On a seasonal (intra-annual) scale, above-ground biomass production occurs through leaf growth, reaching maximum length in summer and minimum in winter. Over the years, many models of varying complexity have attempted to reproduce the growth of marine seagrasses by developing growth curves for leaves during different seasonal periods (Ott (1980)), utilizing the concept of architecture in terrestrial plants for rhizome branching (Molenaar et al. (2000)), using temperature to stimulate only above-ground biomass growth (Zupo et al. (1997)), or considering growth in other plant compartments (leaves, rhizomes, and epiphytes) by incorporating light and nutrient availability (Elkalay et al. (2003)). In this context, the RENOVATE project, funded by the Port System Authority of the Northern-Central Tyrrhenian Sea, aims to develop an ecosystem approach for managing and implementing compensation and mitigation measures in the Sites of Community Importance (SCI) for the coastal strip around the Civitavecchia port, in the Northern Tyrrhenian Sea. The project focuses on restoring the ecosystem services provided by natural habitats, such as *PO* and coralligenous substrates, which have been diminished or altered by anthropogenic pressures in the study area (Marcelli et al. (2023)). Such effort aids in identifying optimal coastal restoration solutions, supported by the numerical model, and enhances coastal resilience against extreme wave events.

This research utilizes a numerical modeling framework to capture the flexibility and seasonal dynamics of *PO*. Through targeted data collection, we enriched our modeling framework with: (i) a detailed characterization of the phenotypic traits based on substrate types in which the seagrass thrives, and (ii) incorporation of seasonal variability in canopy height, by estimating and imposing annual growth and fall of *PO* leaves. To the best of our knowledge, this marks the first study of its kind to validate the numerical model's response using high-resolution local vegetation data, serving as a foundational step toward developing a Coastal Digital Twin in support of NBS, enabling future exploration of coastal management strategies to adapt to and mitigate the impacts of climate change.

The remainder of this paper is structured as follows. Section 2 outlines the modeling framework and its implementation, followed by the model setup for an idealized test case. Section 3 presents a case study in the Civitavecchia coastal strip, where advancements in modeling plant flexibility and seasonal effects are tested in a realistic scenario using a high-resolution domain of up to 20 meters over the vegetated canopies. The main results of these advancements are then presented in Section

https://doi.org/10.5194/egusphere-2025-321
Preprint. Discussion started: 3 February 2025
© Author(s) 2025. CC BY 4.0 License.

4, including the validation against wave buoy data and the investigation of wave attenuation induced by seagrass meadows over the SCIs. The overall discussion (5) and conclusions (6) are then reported in the final sections of the manuscript. Further possible improvements and limitations of the model are also discussed.

2 Modeling framework

The core model utilized in this study is WAVEWATCH III, WW3 (WW3DG, 2019), wind wave model, which solves the action density balance equation for the direction and wave number spectrum (Eq. 1).

$$\frac{\partial N}{\partial t} + \nabla_x \cdot \dot{\mathbf{x}} N + \frac{\partial}{\partial k}\dot{k}N + \frac{\partial}{\partial \theta}\dot{\theta}N = \frac{S}{\sigma} \tag{1}$$

The wave action is a function of the energy spectrum, $F(k,\theta,t,x)$, and intrinsic frequency, σ. x is a two-dimensional space, either in Cartesian, or spherical coordinates, over which the wave action is advected at group velocity relative to the mean current, $\dot{\mathbf{x}} = c_g + U$, with the rate of change in spectral space, $\dot{k}$ and $\dot{\theta}$.

WW3 has been used worldwide from global to coastal applications in both standalone and coupled versions. The modified version of WW3 implemented by Pillai et al. (2022), who incorporated the dissipation source term due to rigid vegetation, served as the foundation for the further advancements in this work. To better model the intricate dynamics of the coastal region at finer resolutions and complex geometry, an unstructured grid configuration was employed. The acronyms and symbols used throughout the paper can be found in A.

The vegetation term is incorporated into the model by augmenting the bottom dissipation source term, S_{bot}, given by a simple empirical linear JONSWAP parametrization (Hasselmann et al. (1973)), as defined in Eq. 2.

$$S_{bot}(k,\theta) = 2\Gamma \frac{n-0.5}{gh} N(k,\theta) + S_{ds,veg} \tag{2}$$

The simplest approach to account for vegetation wave damping effect in a wave model is the equation proposed by Dalrymple et al. (1984) and Mendez and Losada (2004) and adapted in a spectral form by Suzuki et al. (2012) (Eq. 3).

$$S_{ds,veg} = -\sqrt{\frac{2}{\pi}} g^2 \tilde{C}_D b_v N_v \left(\frac{\tilde{k}}{\tilde{\sigma}}\right)^3 \frac{\sinh^3(\tilde{k}l_v) + 3\sinh(\tilde{k}l_v)}{3k\cosh^3(\tilde{k}h)} \sqrt{E_{tot}} E(\sigma,\theta) \tag{3}$$

This formulation models vegetation as rigid leaves and has been utilized in a number of studies (Gupta et al. (2020), Pillai et al. (2022), Abdolali et al. (2022), Jacob et al. (2023)). Several alternative formulations have been proposed to address the overestimation of wave damping. Some of these formulations utilize a drag coefficient that depends on hydrodynamic conditions, such as the Reynolds number or the Keulegan-Carpenter number, as recently described by Abdolali et al. (2022). Another approach is based on plant motion. Our study adopts the latter, specifically by implementing the formulation proposed

https://doi.org/10.5194/egusphere-2025-321
Preprint. Discussion started: 3 February 2025
© Author(s) 2025. CC BY 4.0 License.

by Luhar and Nepf (2011). In this approach, the flexibility effect is incorporated into the source term computation by replacing the vegetation length, l_v, with an effective length, l_e, as a function of the bottom orbital velocity, U_b, according to Eq. 4.

$$l_e = l_\nu - \frac{1 - 0.9Ca^{-1/3}}{1 + Ca^{-3/2}(8 + B^{3/2})} l_\nu \tag{4}$$

where $B = \frac{(\rho - \rho_\nu) g b_\nu t_\nu l_\nu^3}{EI}$,

$Ca = 0.5 \frac{\rho C_D b_\nu U_b^2 l_\nu^3}{EI}$,

$I = \frac{b_v t_v^3}{12}$.

2.1 Idealized test case

Table 1. Numerical model parameters used in the idealized test case.

Bathymetry	Derived from Infantes et al. (2012)
Plants	*PO*
Leaf length l_v	80 cm
Shoot density N_v	615 m^{-2}
Elastic module E	0.47 GPa
Thickness t_v	0.0003 m
Tissue density ρ_v	900 kg m^{-3}
Leaf width b_v	0.0092 m
Simulation period	2009/07/12 - 2009/07/20
Forcing	Wave energy spectrum at the open boundary from Infantes et al. (2012). No winds.
Initial conditions	At rest

To validate the bottom vegetation effects described in 3 and 4, we developed an idealized test case based on the study by Infantes et al. (2012). This study represents a crucial benchmark as it involved a measurement campaign of SWH over *PO* meadows in the Balearic Islands. Additionally, they provided fundamental data on beach depth profiles, *PO* parameters (i.e. shoot density, leave length, meadow extensions), and wave height attenuation along a transect. Our validation methodology aimed to replicate the conditions described in Infantes et al. (2012) within our numerical model implementation. The numerical setup is summarized in Table 1.

The domain of the test case (Figure 1) was reconstructed using an unstructured mesh with a horizontal resolution of approximately 20 meters, extending 1.2 km radially from the shore and 0.7 km along the coastline. The extent and coverage of the vegetation meadows were chosen to reflect the real domain investigated in Infantes et al. (2012), preserving the locations of the moorings, distances from the coast, and distances between moorings. The depth profile and simulation time window were

https://doi.org/10.5194/egusphere-2025-321
Preprint. Discussion started: 3 February 2025
© Author(s) 2025. CC BY 4.0 License.

derived from the original work. To minimize uncertainty from external forcing and to investigate vegetation-induced wave dissipation more accurately, we excluded wind forcing from the simulation. Only the measured wave height time series at the offshore mooring location was imposed at the open lateral boundary (indicated in red in Figure 1) of the test case domain. This boundary forcing represented the only input for our validation test case. The wave direction was assumed to be perpendicular to the coastline.

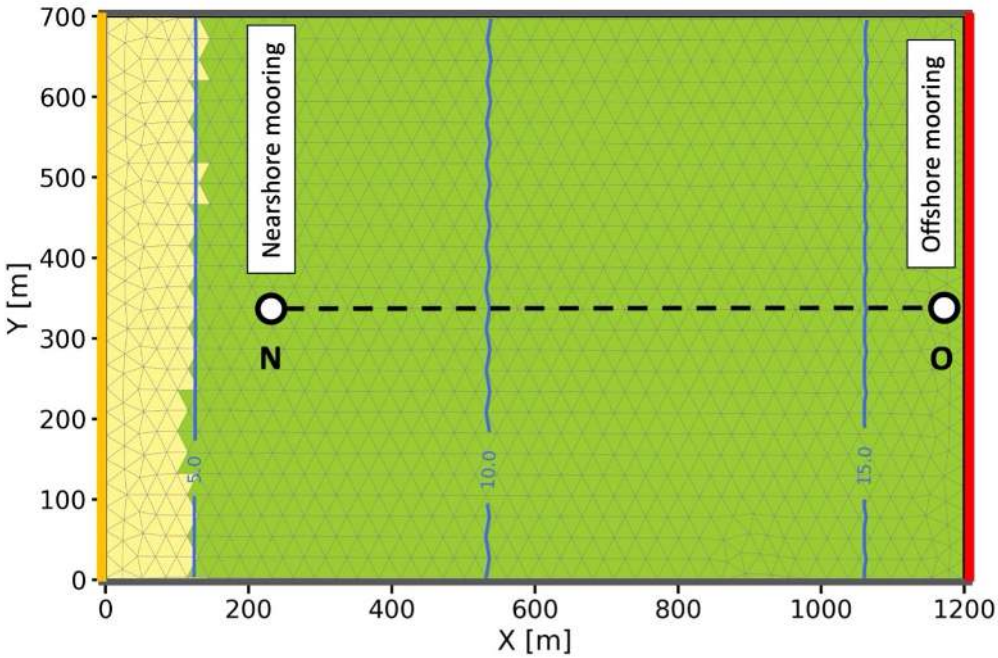

Figure 1. Idealized test case (domain and bathymetry) customized from Infantes et al. (2012), with location of mooring data. *O* denotes offshore moorings, while *N* denotes nearshore moorings. Green mesh elements indicate elements with vegetation, while yellow elements do not include vegetation at the bottom. The dashed line represents the transect *N-O* analyzed later.

We conducted three numerical experiments with the following configurations: *(i)* no vegetation (*no_veg*), using the default code of WW3; *(ii)* rigid vegetation (*veg_rigid*), including the implementation used in Pillai et al. (2022); *(iii)* flexible vegetation (*veg_flex*), including the formulation proposed in this study. The assessment of wave attenuation was carried out by comparing the simulation results with wave measurements taken by Infantes et al. (2012) at a nearshore buoy after the waves traveled approximately 1 km over the vegetation.

Figure 2 presents the results of the test case validation for the period investigated by Infantes. According to the observations, the reduction in wave height, considering the combined effects of vegetation and depth-induced damping, is approximately 50-60% over a distance of ∼1 km.

https://doi.org/10.5194/egusphere-2025-321
Preprint. Discussion started: 3 February 2025
© Author(s) 2025. CC BY 4.0 License.

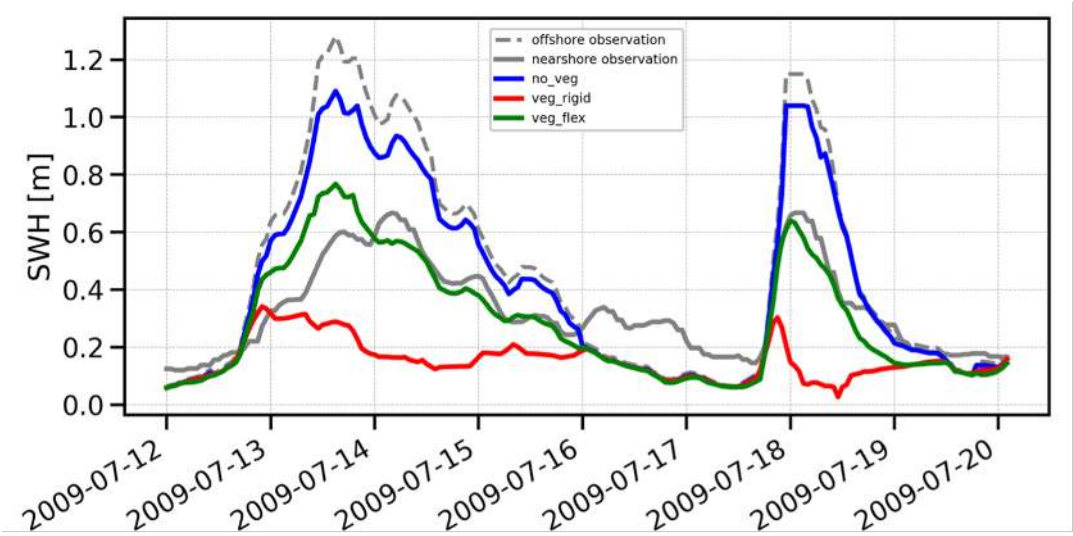

Figure 2. SWH timeseries comparison for *no_veg, veg_rigid* and *veg_flex* experiments against moorings in the idealized geometry of Figure 1.

The three colored lines represent our numerical experiments. As expected, the *no_veg* experiment (blue line) closely mirrors the offshore SWH, as it only accounts for depth-induced dissipation. This low dissipation from offshore to nearshore can be approximately quantified as 10-20% under the simulation conditions. In contrast, the *veg_rigid* experiment (red line) exhibited the greatest wave damping, with very low variability in wave height during the simulation time and a substantial wave reduction of around 80%. The *veg_flex* experiment (green line) provided the highest accuracy (dissipation of ∼40-50%), closely matching the observed peaks and demonstrating good alignment with the observed data.

Figure 3 presents a map *(a)* and transect profile *(b)* of SWH, illustrating wave attenuation during the peak event on 07/17 at 23:00. The offshore observation recorded the wave of 1.2 m, which decreased to 0.65 m at the nearshore station, indicating 50% wave dissipation due to the presence of vegetation and shoaling. This pattern is also captured by the *veg_flex* simulation. The investigation suggests that the attenuation effect is amplified with increased wave height, consistent with the equations 3 and 4.

It is noteworthy that the SWH slopes in the N-O transect of Figure 3b exhibits varying degrees of reduction in the different cases. The *no_veg* simulation showed almost a SWH linear decrease with a very low slope leading to a significant overestimation of SWH. The rigid vegetation simulation (*veg_rigid*) curve shows a linear and rapid drop in SWH as the wave propagates from the boundary over the seagrass meadows. In contrast, the *veg_flex* implementation displays non-linearity as waves approach the shore, attributed to the variation in effective vegetation length in response to different wave energies. All these considerations converge in determining a greater difference between *no_veg* and *veg_flex* simulations as the SWH increases.

https://doi.org/10.5194/egusphere-2025-321
Preprint. Discussion started: 3 February 2025
© Author(s) 2025. CC BY 4.0 License.

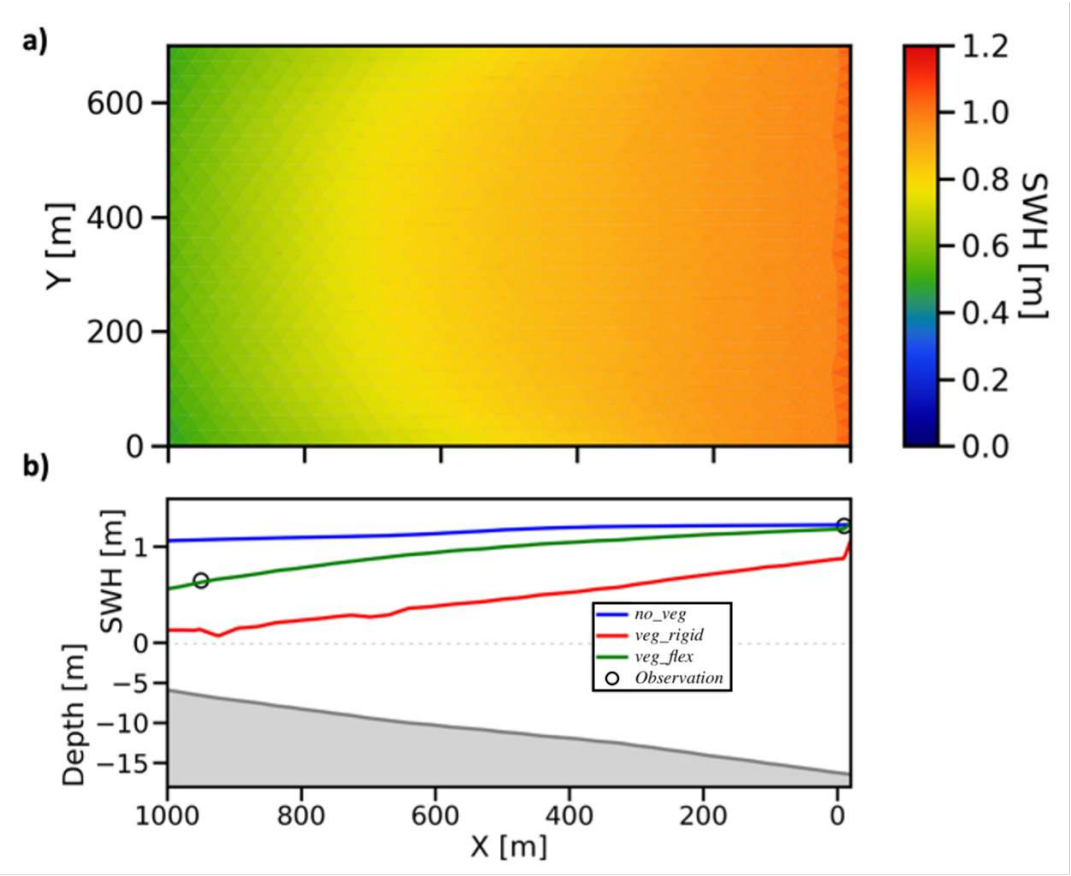

Figure 3. (a) Map of SWH for *veg_flex* configuration and (b) SWH profiles for the three configurations (*no_veg*, *veg_rigid* and *veg_flex*) along the transect N-O (as indicated in Figure 1) at the event peak of 2009-07-17 - 23:00.

Given the high accuracy demonstrated by the flexible vegetation simulation set-up in the idealized case, this model structure is further used in a realistic model setup, considering the coastal area of Civitavecchia along the Latium coast of the Tyrrhenian Sea.

3 The realistic study case

To analyze the attenuation of the waves due to *PO* in realistic conditions, the model was implemented in the coastal area of the northeastern Tyrrhenian Sea, Italy, extending from Tarquinia in the north to S. Severa in the south, with Civitavecchia in central zone of the domain (Figure 4).

The study area contains four SCIs established by the European Union's Habitat Directive (92/43/CEE) under Annex 1. Moving from north to south, the SCI 6000004 ("Seabeds between Marina di Tarquinia and Punta delle Quaglie"), SCI 6000005 ("Seabeds between Punta S. Agostino and Punta Mattonara"), SCI 6000006 ("Seabeds between Punta del Pecoraro and Capo

https://doi.org/10.5194/egusphere-2025-321
Preprint. Discussion started: 3 February 2025
© Author(s) 2025. CC BY 4.0 License.

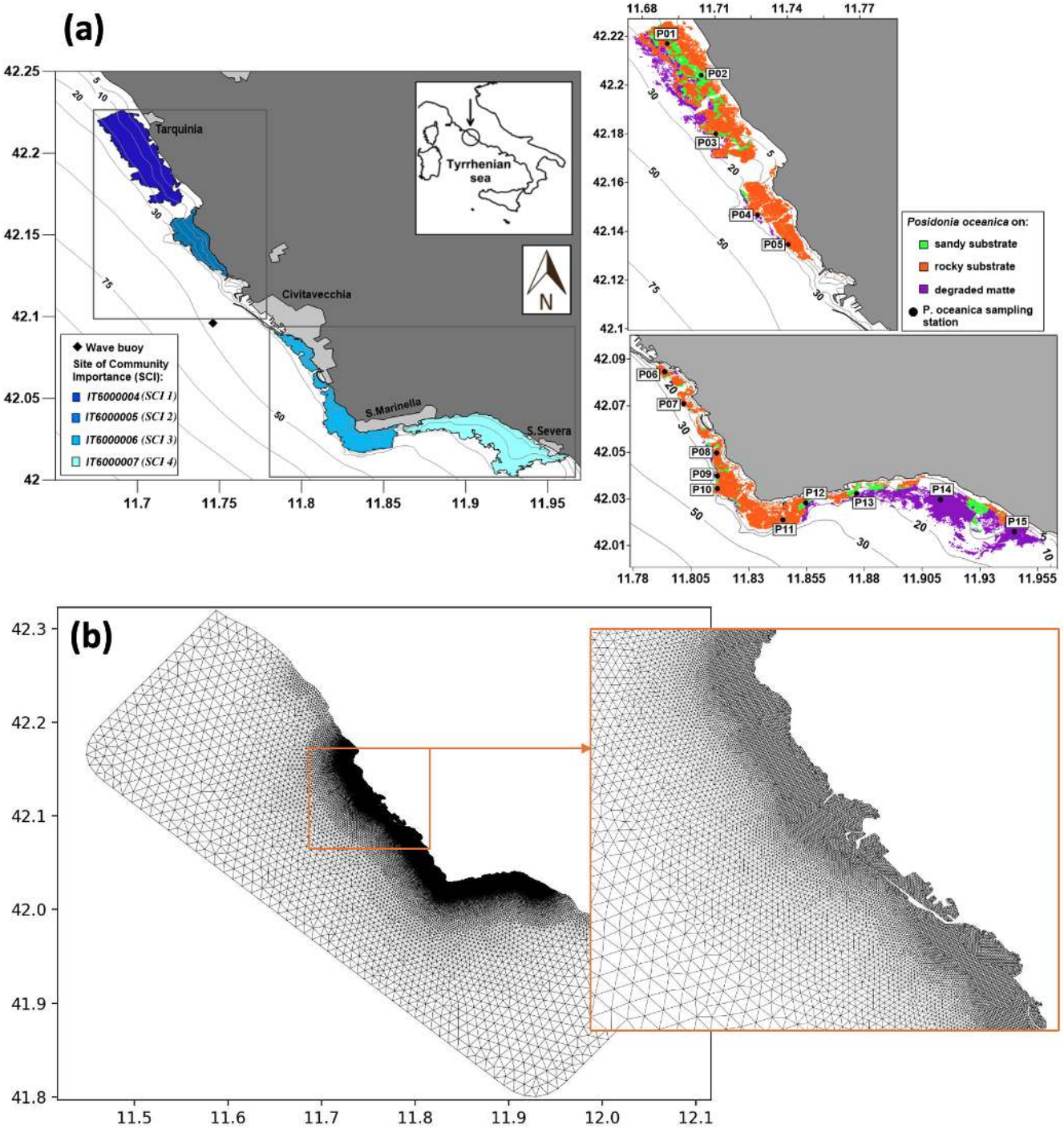

Figure 4. Map of the area of Civitavecchia with bathymetry, Sites of Community Importance (SCI), observations used in the study and distribution of the *Posidonia oceanica (PO)* over the different substrate types (*PO* on rock, *PO* on sand and matte, and degraded matte with *PO*). (b) Mesh of the computational domain with enlarged views in the vicinity of the Civitavecchia harbour.

https://doi.org/10.5194/egusphere-2025-321
Preprint. Discussion started: 3 February 2025
© Author(s) 2025. CC BY 4.0 License.

Linaro"), and SCI 6000007 ("Seabeds off Santa Marinella") are present, hereinafter referenced as SCI 1, SCI 2, SCI 3, and SCI 4 respectively (Figure 4a).

In this area, the *PO* meadows exhibit a discontinuous distribution and high variability in structural and functional descriptors (Figure 4a), reflecting the heterogeneity of the local environments and the presence of various socio-economic activities (Gnisci et al. (2020), Bonamano et al. (2021)). The upper depth limit of *PO* meadows was determined using high-resolution remote sensing imagery (Borfecchia et al. (2019)), while in the shallower depths acoustic surveys (Ardizzone et al. (2018)) have been used. *PO* occur at depths ranging from 0.5 m to 25 m and are situated on rocky substrates (depicted by the brown area in Figure 4a on the right), degraded matte, indicating sediment-rich areas with reduced plant cover and dead matte with isolated patches of *PO*, (the violet area in Figure 4a on the right), and sandy bottoms (the green area in Figure 4a on the right). These meadows exhibit high fragmentation and display significant variability in coverage, ranging from 6% to 98%, with a coefficient of variation of 72.4% (Gnisci et al. (2020)). Moreover, the density is influenced by the meadows' architecture, with an average of 141.7 $\pm$ 62.9 shoots per square meter (Bonamano et al. (2015); Gnisci et al. (2020)). The lack of specific management plans for SCIs, such as ecofriendly buoys to prevent anchoring of recreational boats on *PO* meadows, anti-trawling barriers to deter fishing boats from using nets within SCIs, and an early warning system for dredging and accidental hydrocarbon spills, renders *PO* vulnerable to various anthropogenic stressors present in the study area. Urban and industrial discharges from aquaculture and power plants, the presence of an oil platform, trawling activities, and harbor activities connected to Civitavecchia port have significantly impacted the health of the meadows.

3.1 Model setup

Spanning approximately 90 km along the northeastern Tyrrhenian Sea coast, the model domain (Figure 4b) is centered around the port of Civitavecchia. Coastline reconstruction involved integrating data from recent high-resolution satellite images with the OpenStreetMap dataset (OpenStreetMap contributors (2017)). Advanced, customized meshing tools were employed to achieve a high grid resolution of around 20 m near the shore and a coarser resolution of approximately 2 km offshore. GMSH (Geuzaine and Remacle (2009)) was utilized for mesh generation, while BLENDER (Blender Community (1994)) facilitated optimization and quality checks of the triangles (Bonamano et al. (2024)). The meshing algorithm, based on a frontal Delaunay approach (Remacle et al. (2013)), defines the nominal grid size as the maximum edge length of the triangles.

Bathymetric data were obtained from the EMODNET product (Consortium (2016)) at a resolution of 1/8 × 1/8 arc-min (approximately 230 × 230 m) for the open sea. This data was augmented with high-resolution multi-beam data collected in specific coastal areas, including near the harbor area and within the SCIs, provided by the Autorità di Sistema Portuale del Mar Tirreno Centro Settentrionale. At the open lateral boundaries, the domain is forced with the downscaled Copernicus regional model (Korres et al. (2023)) mean wave parameters (H_s, θ, T_{peak}) of 1h frequency for the period of simulation of 1 year (2016/10/01 – 2017/09/30). ECMWF operational analysis (Owens and Hewson (2018)) were used for wind data at 6h frequency. The specific parametrizations for the WW3 model set-up are summarized in A.

To assess the wave attenuation in the study area, we conduct three experiments with different parametrizations in the vegetation module (Table 2). In the first configuration, we simulated the absence of the meadows in the study area by excluding

https://doi.org/10.5194/egusphere-2025-321
Preprint. Discussion started: 3 February 2025
© Author(s) 2025. CC BY 4.0 License.

Table 2. Description of the numerical experiments.

Experiment	Configuration	Description
NV	No vegetation	The simulation is conducted without any vegetation present.
VF	Flexible vegetation with varying substrates	The simulation incorporates flexible vegetation with annual mean leaf length values for *PO* (l_{av} as shown in Table 3). Spatial variations in leaf length and shoot density are accounted for based on substrate types (rock, sand, and degraded matte).
VFS	Flexible vegetation with varying substrates and seasonal growth factors	This simulation captures the seasonal growth of *PO*, as depicted in Figure 5. Initial values (l_v) for October 2016 are provided in Table 3. Growth and shoot density vary across substrate types (rock, sand, and degraded matte).

Table 3. Vegetation parameters for different substrates of *PO* meadows with initial and averaged over the simulation period (annual mean) leaf length values.

PO parameters	Rock	Sand and Matte	Degraded Matte
N_v (m^{-2})	209.46	277.57	145.3
l_v (cm)	47.5	46.3	41.2
l_{av} (cm)	28.5	35.8	25.5
b_v (cm)	0.92	0.92	0.92
t_v (cm)	0.03	0.03	0.03
ρ_v (kg/m^2)	218.6	218.6	218.6
E (GPa)	0.47	0.47	0.47

the source term $S_{ds,veg}$. In the second configuration, VF, all the parameters of the vegetation module remain constant over time, while leaf length and shoot density vary according to different substrate types, therefore mimicking the growth dynamics in the model (Table 3). The values for leaf length and shoot density represent the annual average derived from inter-annual sampling (see Section 3.2). The elastic module value is set at 0.47 and was determined by Folkard (2005), who measured the angle of deflection of a small, cantilevered strip of the sheeting when loaded with small weights. In the third configuration, VFS, the model mimics the seasonal variations in canopy height, defined as the maximum length of a leaf within a shoot. This is achieved by fitting a fifth-degree polynomial curve to canopy height data collected in *PO* meadows within the study area. The growth curves obtained for the three substrate types 5 exhibit a trend similar to those described by Ott (1980) in Gulf of Naples, an area in the Thyrrenian Sea close to the current study area with similar wave climate. A similar approach has already

https://doi.org/10.5194/egusphere-2025-321
Preprint. Discussion started: 3 February 2025
© Author(s) 2025. CC BY 4.0 License.

been employed in previous studies to analyze the annual growth dynamics of *PO* (Duarte (1989); Alcoverro et al. (1995)) and to estimate the carbon dioxide fixed by the plants (Vassallo et al. (2013)).

According to this growth model, maximum leaf growth is reached at the end of the summer period. Subsequently, intense autumn storms cause the detachment of older leaves, resulting in a sharp reduction in canopy height during winter, leaving only juvenile leaves at their minimum annual length. Specifically, in the study area, the growth of *PO* on sandy substrates occurs more rapidly compared to other substrates, resulting in generally longer leaves during the summer period. Conversely, canopy height is lower for *PO* growing on degraded matte, as the reduced shoot density offers limited protection against intense autumnal storms, which tend to uproot nearly all leaves, leaving only those a few millimeters long. Thus, the values shown in Table 3 for initial leaf length reflect initial conditions of *PO* meadows in October and are subject to change over the simulation according to Figure 5 for VFS experiment.

While the growth factor is inherently site-specific and influenced by physical variables such as wave action, turbidity, temperature, and proximity to river mouths requiring localized data collection, the proposed formulation offers a significant advantage: it eliminates reliance on abiotic parameters like temperature, light, and nutrients. These parameters often face challenges such as limited temporal coverage (e.g., cloud cover disrupting high-resolution satellite observations) or insufficient spatial resolution in coastal zones (e.g., the 4 km grid used by Copernicus Marine Services regional models).

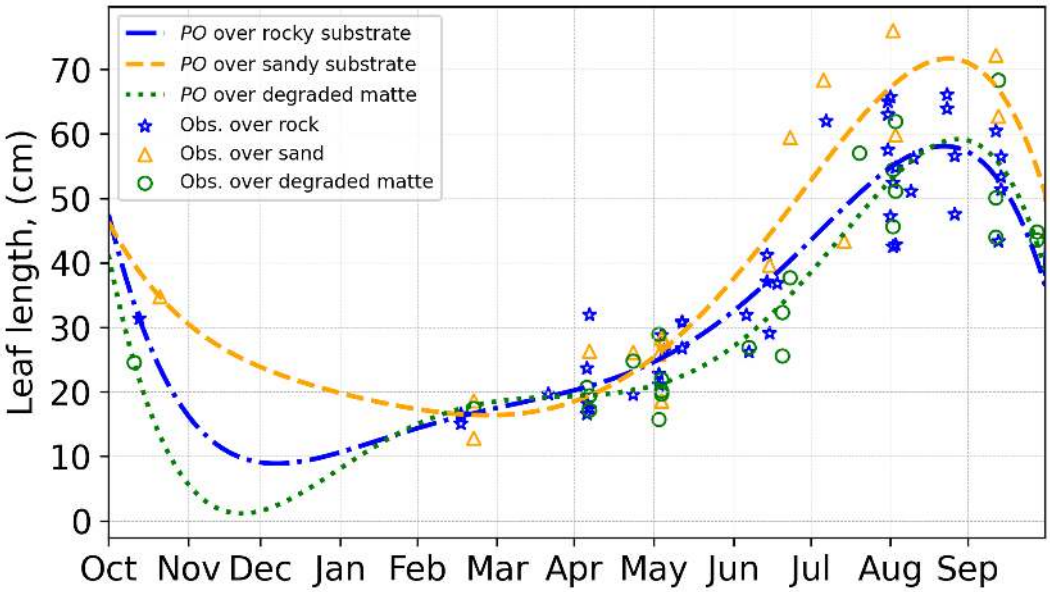

Figure 5. Timeseries of *PO* leaves height variation throughout the year, showing seasonal observations alongside fitted growth curves.

https://doi.org/10.5194/egusphere-2025-321
Preprint. Discussion started: 3 February 2025
© Author(s) 2025. CC BY 4.0 License.

3.2 Observational data

To model the *PO* meadows in the four SCIs, structural, morphological, and dynamic parameters of the seagrass were collected at 15 stations (POS1-POS15) in 2017, as illustrated in Figure 4a on the right. The sampling of plants followed a hierarchical design in accordance with the standard protocol reported in Buia et al. (2004). By scuba diving, shoot density, N_v, was determined as shoots per square meter by counting the number of shoots within nine randomly selected squares (40 × 40 cm). A total of 18 orthotropic rhizomes were randomly collected from each station (six rhizomes for three replicates per station) for phenological analysis (Giraud et al. (1979)). In the laboratory, leaves of *PO* were scraped to remove epiphytes and then washed in distilled water. Subsequently, biometric variables such as the number, length (l_v), width (b_v), and thickness (t_v) of juvenile, intermediate, and adult leaves per shoot were measured at each station, following Giraud's classification (Giraud (1977)). According to Pergent-Martini et al. (2021), the longest leaf within a shoot is most often the third-ranked leaf, which has therefore been adopted as the representative value for canopy height. To calculate the tissue density of the leaves (ρ_v), the oldest leaf with an intact apex was dried in an oven at 60^oC for 48 hours and then weighed. Leaf density was then estimated by dividing the dry weight of the leaf by its volume, calculated from the previously defined biometric data.

To validate the WW3 model, wave data were gathered from the wave buoy of the Civitavecchia Coastal Environment Monitoring System (C-CEMS), developed by the Laboratory of Experimental Oceanology and Marine Ecology and operational since 2005 in the coastal marine area of Civitavecchia (Bonamano et al. (2016); Bonamano et al. (2021); Bonamano et al. (2023)). The Datawell wave buoy is equipped with a wave motion sensor mounted on a stabilized platform, along with accelerometers and a magnetic compass. It has enabled the measurement of wave height (with an accuracy of 0.5% of the measured value), wave direction, wave period at a depth of approximately 50 meters. The simulations were validated using SWH measurements recorded from October 2016 to November 2017.

4 Results

In this section, we first analyze the wave fields over the Civitavecchia region (Section 4.1) based on VFS configuration results and discuss the overarching wave patterns. Subsequently, in Section 4.2, we validate the VFS experiment output against observational data, evaluating the performance metrics such as correlation coefficient and bias. In Section 4.3 we intercompare the VF and VFS experiments against the NV.

4.1 Wave field analysis

The area of Civitavecchia is influenced by the waves approaching predominantly from southwest as shown on an annual mean SWH, Figure 6 (a, b). In VFS configuration, the waves are impacted by the vegetated zones producing irregular SWH patterns along the coast. The deep blue color depicts the harbor zone, which is shielded by the breakwater. The patches of light blue regions, in (a), show the annual mean wave height reduction due to the presence of vegetation down to 0.2 m from 0.4 m in NV configuration, (b). The seasonal SWH maps (Figure 6 c, d, e, f) illustrate that waves are greater during autumn to winter

https://doi.org/10.5194/egusphere-2025-321
Preprint. Discussion started: 3 February 2025
© Author(s) 2025. CC BY 4.0 License.

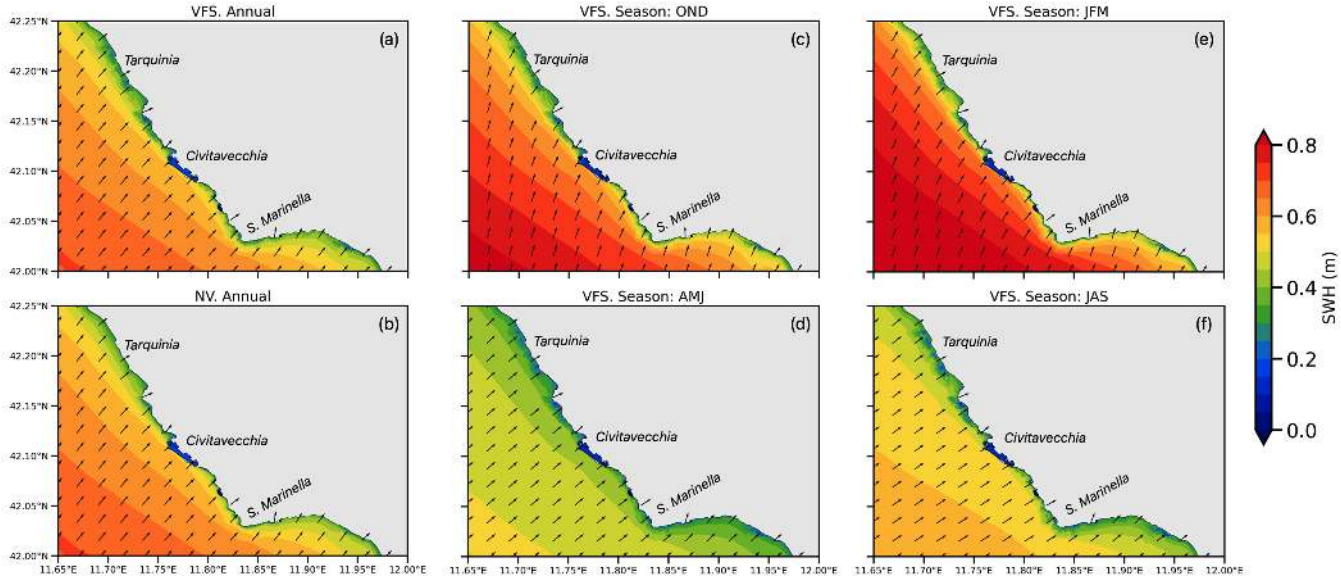

Figure 6. Maps (zoomed over the coastal area) of annual mean (a) and seasonal (OND, JFM, AMJ, JAS) mean (b, c, d, e) SWH (1 Oct 2016 - 30 Sept 2017) including flexible vegetation and seasonality effect (VFS).

period (OND, JFM), with offshore waves averaging 0.8 m and diminishing to 0.4 m at the coast of Civitavecchia. During this period, the predominant wave direction is northward, highlighting the exposure of site SCI 3 to substantial wave activity at the Santa Marinella coastal edge. Conversely, during the warmer spring to summer period (AMJ, JAS), wave energies decrease by $\sim$ 40%, with offshore waves averaging 0.5 m and reducing to 0.3 m at the coast. During this period, the waves approach the coast more perpendicularly and SCI 4 benefits from the partial protection provided by the Santa Marinella headland, resulting in wave divergence.

4.2 Model validation

The SWH timeseries in Figure 7a at the wave buoy location (see Figure 4a) provides insight into high-amplitude waves over the simulated periods, with wave heights reaching 4 meters, peaking in March. Similarly, we can conclude here that such strong events occur more frequently in colder seasons. As previously noted, we anticipate that high-amplitude waves in autumn will impact the coastline and significantly damage the vegetation canopies starting over the seasonal cycle in October, as observed in Figure 7a. The figure compares the VFS experiment results with wave observations collected during the same period, represented in red. To minimize the impact of extreme point-wise variations or shifts, the average values from the five nodes closest to the buoy were used. The model generally overestimates wave heights during autumn and winter, while slightly underestimating peak wave events in spring and summer. When wave heights are below 0.5 m, the model tends to provide lower estimates than observed. Overall, the model demonstrates strong performance, accurately capturing peak events with a high correlation coefficient of 0.95 and a bias of -0.14 m (Figure 7b).

https://doi.org/10.5194/egusphere-2025-321
Preprint. Discussion started: 3 February 2025
© Author(s) 2025. CC BY 4.0 License.

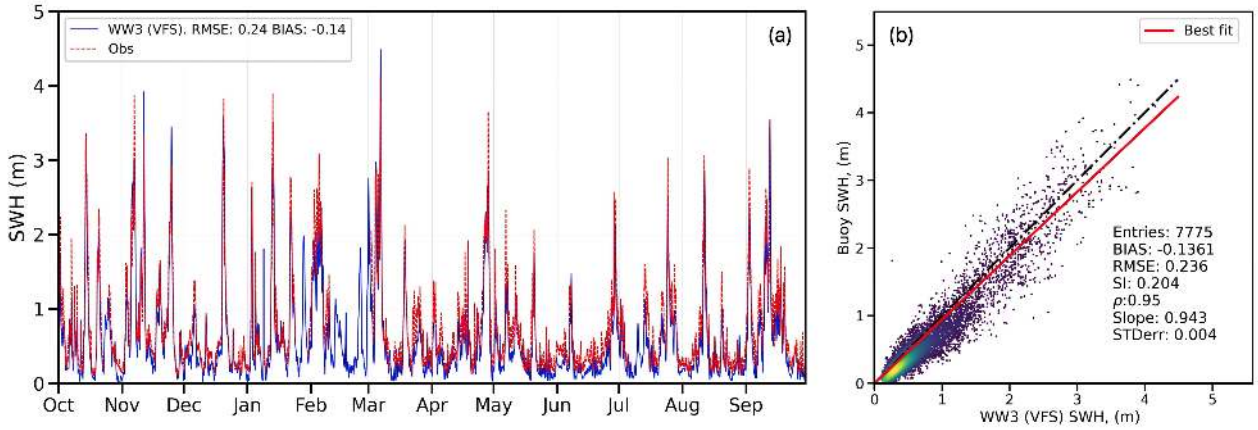

Figure 7. Comparison of the model results (VFS) with the buoy data (Figure 4a) in terms of timeseries (a) and a scatter plot (b).

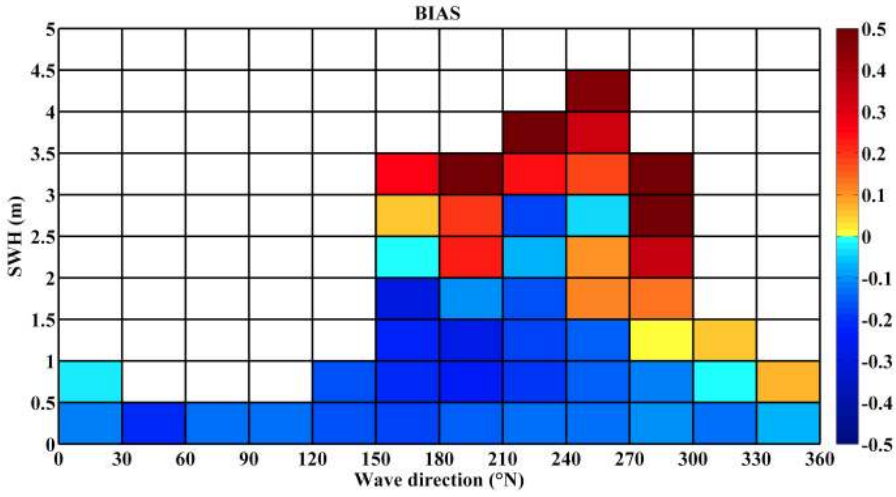

Figure 8. SWH and wave direction bias heatmap (m).

We further analyze the model performance calculating the bias in SWH associated with the incoming wave direction (Figure 8). Consistent with the quiver map in Figure 6a, the mean incoming wave direction is southwest, ranging between 210–240°N. We see a positive increase in SWH bias with increasing wave height, reaching up to 0.5 m for waves with magnitudes of 3 – 4.5 m. However, for smaller southern waves, 180°N, with the heights of 1 – 2 meters, the model predominantly underestimates SWH, showing a negative bias of up to 0.4 m. The highest positive bias is more frequently observed for the western waves (270–300°N) of 2.5 – 3.5 m magnitude. This variability in bias is likely associated with the absence of coupling effects with currents.

https://doi.org/10.5194/egusphere-2025-321
Preprint. Discussion started: 3 February 2025
© Author(s) 2025. CC BY 4.0 License.

Table 4. Monthly mean SWH and UBR over vegetation area and their differences for the three experiments in Table 2.

Variable	Experiment	OCT	NOV	DEC	JAN	FEB	MAR	APR	MAY	JUN	JUL	AUG	SEP
SWH (m)	VFS	0.421	0.638	0.319	0.456	0.500	0.474	0.423	0.300	0.285	0.358	0.257	0.484
	VF	0.421	0.606	0.305	0.439	0.532	0.461	0.418	0.299	0.288	0.369	0.266	0.508
	NV	0.456	0.671	0.330	0.480	0.583	0.509	0.451	0.317	0.302	0.393	0.280	0.557
SWH (%)	VFS-NV	-7.704	-4.854	-3.366	-4.910	-5.703	-6.841	-6.197	-5.163	-5.832	-8.968	-8.239	-13.084
	VF-NV	-7.809	-9.635	-7.464	-8.569	-8.684	-9.374	-7.251	-5.415	-4.707	-6.184	-5.304	-8.834
	VFS-VF	0.113	5.290	4.428	4.001	3.264	2.795	1.136	0.266	-1.180	-2.967	-3.099	-4.661
UBR (m/s)	VFS	0.096	0.156	0.078	0.105	0.138	0.114	0.095	0.061	0.056	0.078	0.048	0.117
	VF	0.096	0.147	0.074	0.100	0.133	0.111	0.094	0.061	0.056	0.081	0.050	0.123
	NV	0.106	0.165	0.081	0.111	0.147	0.124	0.103	0.066	0.060	0.088	0.054	0.137
UBR (%)	VFS-NV	-9.155	-5.273	-3.799	-5.756	-6.267	-7.559	-7.321	-7.176	-8.157	-11.509	-11.494	-14.632
	VF-NV	-9.218	-10.524	-8.713	-10.214	-9.645	-10.437	-8.582	-7.521	-6.597	-7.954	-7.408	-9.909
	VFS-VF	0.070	5.869	5.383	4.965	3.213	3.213	1.379	0.373	-1.671	-3.862	-4.413	-5.242

4.3 Seagrass induced wave attenuation

We compare the three different experiments, described in Table 2, to estimate the significance and contribution of vegetation and seasonality in wave attenuation. Table 4 summarizes monthly mean SWH and bottom wave orbital velocities (UBR), averaged over all the vegetated nodes for three experiments and their percentage differences. Such vegetated areas' mean values allow us to quantitatively assess the performances of both VFS and VF experiments focusing on the effect of seasonal variation of the canopy. On average, across the domain, the mean monthly wave height varies from 0.2 to 0.6 m, attenuating from 3% in December to 13% in September across all vegetated areas, with similar dissipation rates for UBR. The effect of seasonality accounts for 10% of variation for both SWH and UBR (VFS – NV). Wave energy damping efficiency varies by month, with lower attenuation observed during the early stages of leaf growth (NOV–DEC), where the positive difference between VFS and VF is highest. A negative difference, indicating stronger wave attenuation, occurs when leaf length exceeds the annual average set for the VF simulation (JUN–OCT).

However, this comparison does not capture the impact of specific phenotypic traits, their distinct growth patterns, or wave-energy-dependent dissipation. Therefore, we further analyze the substrate- and node-wise impact of the canopy on wave dynamics, accounting for seasonal variations.

4.3.1 VFS vs. NV: Wave attenuation by *PO* over different substrate types and SCIs

Figure 9 illustrates the cyclic, monthly mean reduction in SWH and UBR throughout the year (Oct'16 – Nov'17), averaged across different phenotypic traits of *PO* and SCIs, attributable to the presence of flexible vegetation canopies with seasonal effect, given by the difference between VFS and NV configurations. As stated earlier, the wave attenuation is a function of seagrass characteristics and wave energy. During the summer months, the leaves undergo rapid growth due to calm seas,

https://doi.org/10.5194/egusphere-2025-321
Preprint. Discussion started: 3 February 2025
© Author(s) 2025. CC BY 4.0 License.

optimal weather and nutrient availability, reaching peak maturity in late summer, followed by the arrival of high waves, which damage the canopies. The observed wave attenuation pattern aligns with the seasonal growth trend shown in Figure 5. In winter, wave height attenuation is at its lowest, ranging from 2% – 9% over all SCIs and 1% – 11% across various substrate types, with the strong variation between *POs* over degraded matte and rocks; similarly for the bottom orbital velocities marking 3% – 8% and 1% – 14% of reduction respectively. From spring through summer, the pattern remains consistent, with average wave reduction around 7% – 9% for both SWH and UBR. This seasonal trend reflects high wave energy and shorter leaf lengths in spring, followed by lower wave energy and developing leaves in summer. When leaf maturity peaks and high waves arrive in September, both factors contribute to maximum wave damping, with reductions of 10% – 18% in SWH over SCIs and 9% – 24% across substrates, and 13% – 20% and 11% – 29% in UBR, respectively. *PO* growing on sandy and rocky substrates demonstrates a more pronounced impact on wave attenuation compared to degraded matte, which is characterized by lower shoot density and leaf length of *PO*.

4.3.2 VFS vs. VF: The contribution of seasonal variability of seagrass leaf length

To isolate the seasonal impact of the vegetation model on wave energy dissipation, we compare the VFS and VF experiments. Figure 10's bar chart illustrates the percentage differences between the two simulations considering the phenotypic traits of *PO*. The seasonal pattern of seagrass growth results in a positive difference, reflecting lower wave damping capacity during late autumn, winter, and spring, and a shift to a negative difference in summer and early autumn, indicating higher wave damping capacity. The maximum seasonal variation reaches around 10%, 16%, and 20% over degraded matte, sand, and rocks, accordingly, for both SWH and UBR. The average seasonal deviation across all substrates is approximately 5% (depicted in orange), as observed earlier in Section 4.3. Overall, the deviation bars adhere to the seasonal growth curves in Figure 5.

4.3.3 VFS vs. NV: Seasonal wave attenuation maps

Figure 11 illustrates the node-wise SWH attenuation capacity of vegetated areas, dependent on wave magnitude. Seasonal reductions in SWH range from 20% to 40% in the SCI 1 and 2 regions (north of Civitavecchia port) and from 10% to 30% in SCI 3 and 4. This discrepancy can be attributed to several factors, such as partial sheltering by S. Marinella headland (Section 4.1), seagrass distribution (Figure 4a), and lower wave damping capacity of *PO* over degraded matte (Section 4.3.1). SCI 2 exhibits the highest wave attenuation capacity, attributed to its predominantly rocky substrate and direct wave exposure. Seasonally, peak wave attenuation occurs during the JAS period (d), driven by intense storm events and the canopy reaching its maximum height. Lower values are observed in winter and spring (a, b, c) due to the presence of predominately juvenile leaves.

5 Discussion

As proposed by Luhar and Nepf (2011), the flexibility effect was incorporated into the source term of WW3 by replacing the vegetation leaf length with an effective length as a function of the bottom orbital velocity. Due to the plant's partial passive

https://doi.org/10.5194/egusphere-2025-321
Preprint. Discussion started: 3 February 2025
© Author(s) 2025. CC BY 4.0 License.

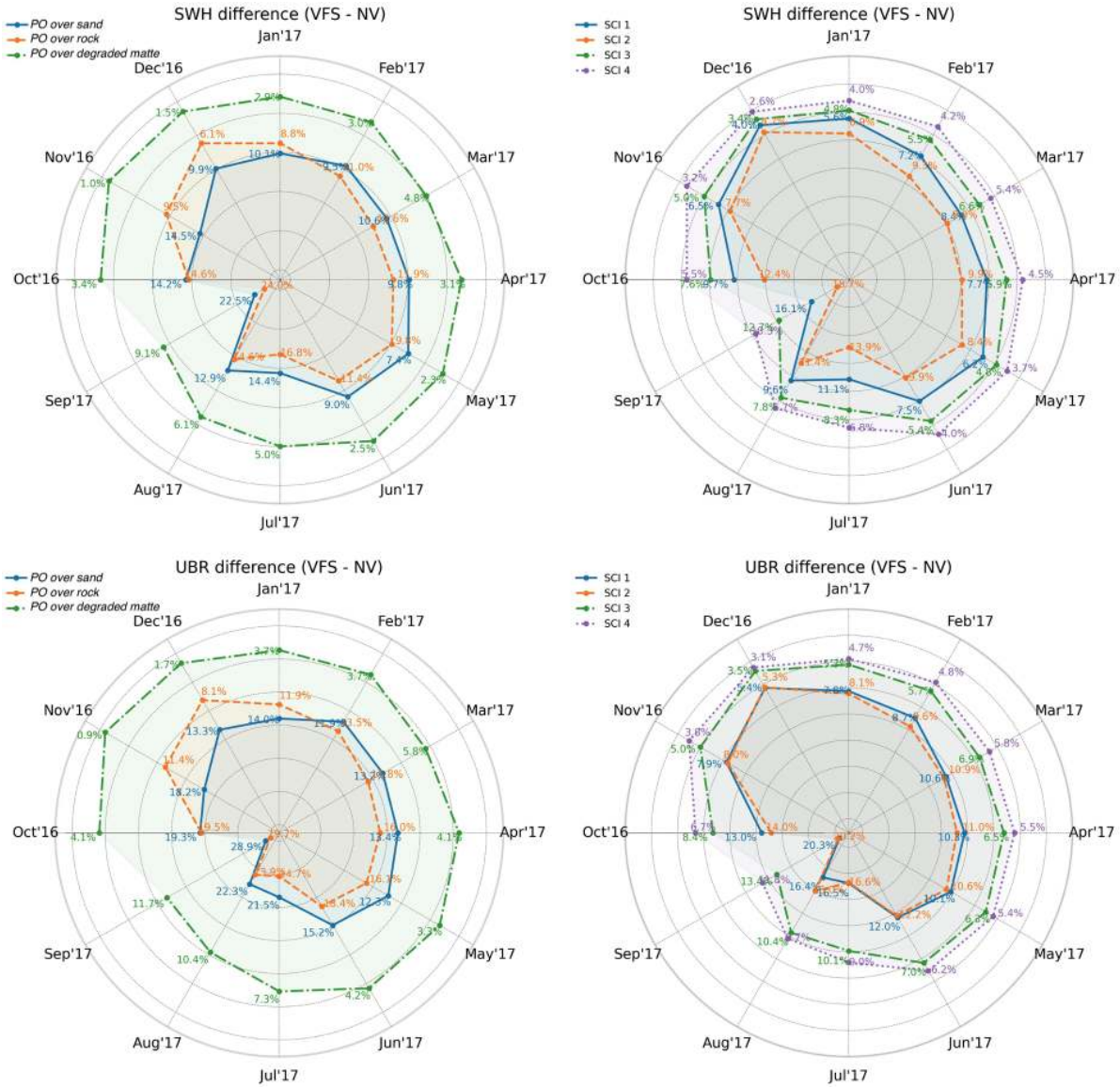

Figure 9. Mean monthly SWH and UBR percentage reduction for VFS configuration for the three different phenotypic traits of *P. oceanica* (over rock, sand, degraded matte), and four SCIs, averaged across vegetated points in the mask.

movement with the wave, this new configuration results in a reduced wave height attenuation compared to that for a fully rigid blade of the same geometry (Lei and Nepf (2019)).

To explore how incorporating flexibility can improve model performance and better simulate the effects of seagrass meadows on wave attenuation, an idealized test case was designed to replicate the experiment of Infantes et al. (2012) in the Balearic Islands, where wave parameters were measured for over a month within a *PO* meadow with known shoot density and leaf

https://doi.org/10.5194/egusphere-2025-321
Preprint. Discussion started: 3 February 2025
© Author(s) 2025. CC BY 4.0 License.

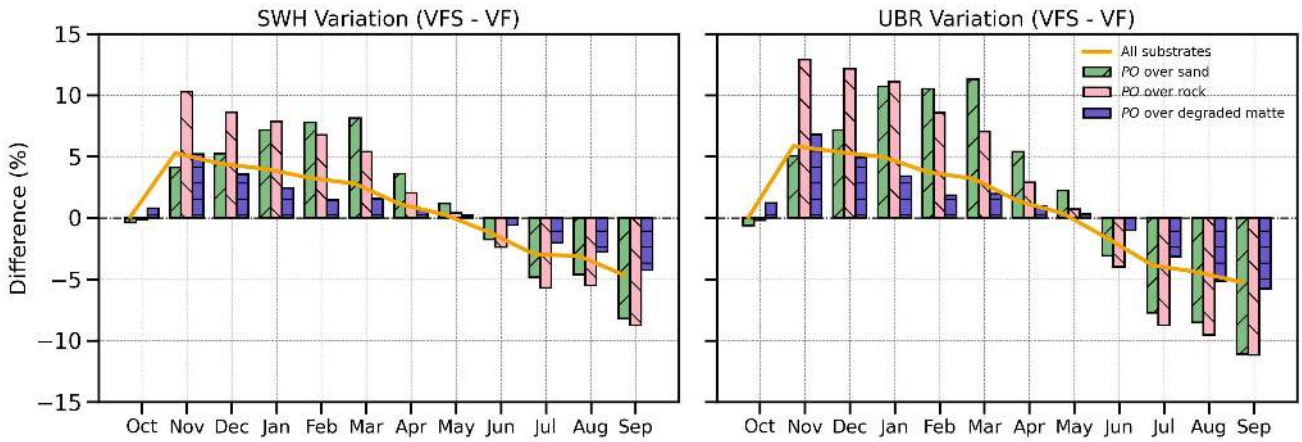

Figure 10. Timeseries of mean monthly SWH and UBR percentage difference between VFS and VF simulations across substrate types, averaged over the vegetation points per substrate in the mask (bars) and over all substrates (orange solid line).

length. The model results demonstrated a markedly improved agreement with observed data, achieving wave damping of up to 40-50% for peak energies, compared to the rigid vegetation experiment, which substantially overestimated it at around 80%. Additionally, the model produced a cross-shore variation of wave height that more accurately mimics the non-linear characteristics inherent in the complex interaction between waves and a flexible canopy.

At seasonal scale, we observed a monthly wave damping deviation of $\pm 5\%$, averaged across *PO* over different substrate types, attributed to the seasonality effect in contrast to the flexible vegetation model alone. Reduced wave dissipation rates were observed until June, when leaf lengths surpassed the annual averages established for each phenotypic trait in the non-seasonal experiment, VF, after which wave damping increased toward the end of the seasonal cycle in September. Thus, the lack of seasonal variability in the model leads to a misrepresentation of seagrass wave damping efficacy, overestimating its impact in winter and spring, and underestimating it in summer and autumn.

From a spatial point of view, in terms of SCI sites, the model showed a wave damping of approximately 10% during peak waves in March for SCI 2 on average. As both SCI 1 and SCI 2 are predominantly composed of rocky substrates and are exposed to direct waves from the southwest, they experience a greater impact and, consequently, more significant wave reduction compared to SCI 3 and SCI 4. The maximum wave damping reached 16% - 18% on average in September over 1st and 2nd sites, and 10% - 12% over 3rd and 4th sites. The seasonal effect did not show a linear correlation with the monthly average wave reduction across SCIs when compared to non-vegetated simulations. This aligns with the vegetation model, where wave dissipation is closely related to both wave energy levels and leaf length. Similarly, we observed consistent results in the analysis of wave damping across various substrate types, with peak SWH reductions of 24%, 22%, and 9% for *PO* traits over rock, sand, and degraded matte, respectively. It's noteworthy that SCI 4, characterized by a higher concentration of degraded matte, exhibited a lower wave attenuation capacity of maximum 10%.

https://doi.org/10.5194/egusphere-2025-321
Preprint. Discussion started: 3 February 2025
© Author(s) 2025. CC BY 4.0 License.

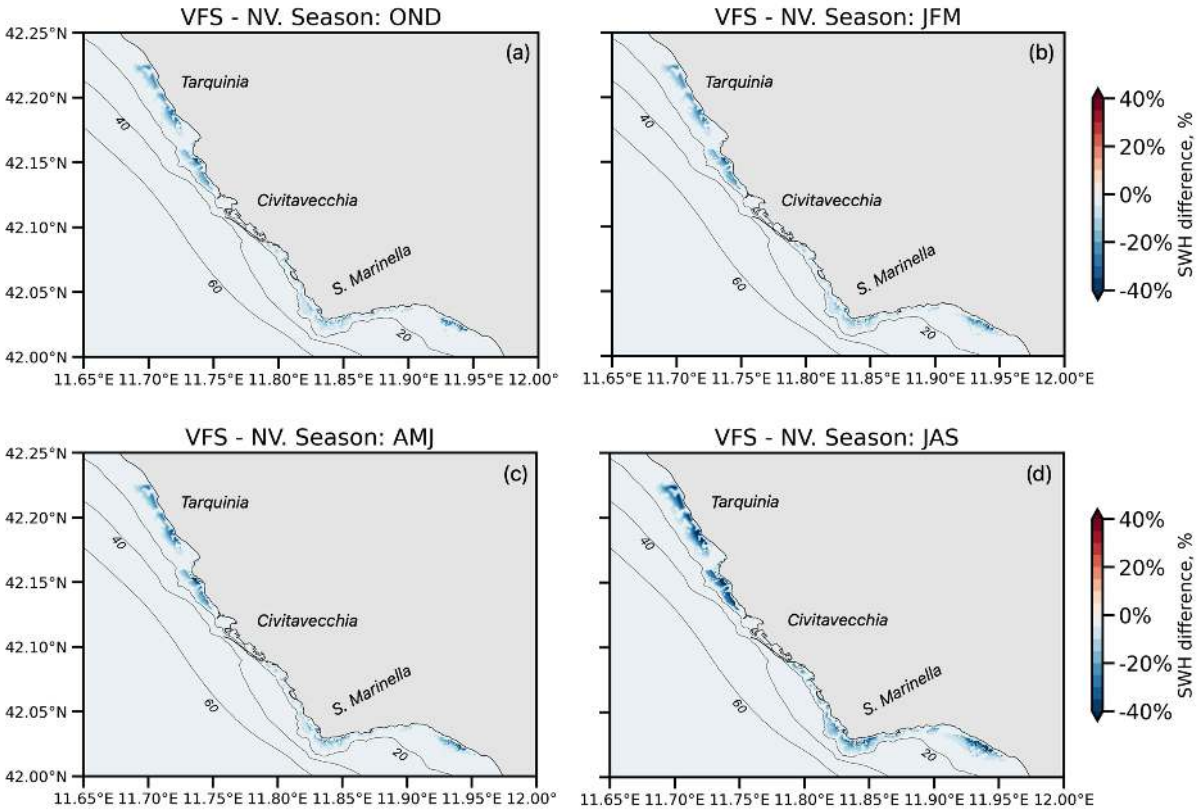

Figure 11. Maps (zoomed over the coastal area) of seasonal (OND, JFM, AMJ, JAS) mean SWH attenuation (VFS – NV).

This research provides a comprehensive analysis of the impact of submerged vegetation on wave propagation in the nearshore zone, aimed at evaluating the role of seagrass as a Nature-Based Solution ((Pillai et al. (2022)); Jacob et al. (2023); Unguendoli et al. (2023)). Additionally, it seeks to enhance the management of Sites of Community Importance (SCIs) by providing insights into wave dynamics to identify optimal areas for restoration activities (Rifai et al. (2023); Pansini et al. (2022); Chen et al. (2024)), thereby maximizing the ecological benefits of such interventions. Among marine phanerogams, *PO* has a high capacity for wave attenuation as it forms extensive and dense meadows in coastal areas, with leaves that frequently exceed one meter in length Koftis et al. (2013). Due to changing wave energies, *PO* meadows bend and straighten, causing varying shear stresses depending on wave orbital velocities. This dynamic interaction reduces shear stresses and leads to a lower wave damping effect, which was accurately replicated with the flexible vegetation model (Luhar and Nepf (2011)).

It is important to note that the seasonality effect is applied to the Civitavecchia site with coefficients empirically derived from site measurements. Consequently, this approach relies on fitted growth curves known for the site of interest, although it can be adapted for use in other areas, provided that the observational data are available. Here, however, the development was specifically tailored to accurately estimate the dynamics of the Civitavecchia coastal region. Seasonal variation was primarily tracked by monitoring the extension of leaf length over time, without considering the decline in size, coverage, and shoot

https://doi.org/10.5194/egusphere-2025-321
Preprint. Discussion started: 3 February 2025
© Author(s) 2025. CC BY 4.0 License.

density in recent decades (Marbà et al. (2014); Telesca et al. (2015)) due to a combination of anthropogenic impacts (i.e., boat anchoring, siltation, etc.) and climate change (i.e., introduction of exotic species, the rise of sea surface temperature, and the intensification of wave energy along the coastal zone). In this context, the application of innovative monitoring techniques, including the use of autonomous vehicles (e.g., Unmanned Surface Vehicles - USVs) equipped with acoustic instrumentation capable of measuring the height and coverage of marine vegetation, would be highly beneficial. These techniques can increase the spatial and temporal coverage of data, provide information on plant characteristics up to a few meters from the shore, and detect seagrass canopy coverage and height changes following significant extreme events (Piazzolla et al. (2024)). Such events can potentially damage vegetation canopies, leading to the temporary absence of seagrass meadows (Oprandi et al. (2020)), thereby reducing the wave attenuation effect. This feedback loop from the wave model to the vegetation dynamics was not incorporated into our model. Furthermore, the sole use of a wave model without considering hydrodynamics means that relying only on near-bed orbital velocities does not account for the shear stresses induced on the vegetation canopy by currents. To make the growth model of *PO* applicable to other coastal areas of the Mediterranean Sea, future evaluations will consider deterministic (Zupo et al. (1997); Elkalay et al. (2003)) and statistical approaches (Catucci and Scardi (2020)).

6 Conclusion

This research provides a comprehensive analysis of the impact of submerged vegetation on wave propagation in the nearshore zone, aimed at evaluating the role of seagrass as a NBS (Pillai et al. (2022); Jacob et al. (2023); Unguendoli et al. (2023)). Additionally, it seeks to enhance the management of Sites of Community Importance by providing insights into wave dynamics to identify optimal areas for restoration activities (Rifai et al. (2023); Pansini et al. (2022); Chen et al. (2024)), thereby maximizing the ecological benefits of such interventions. Among marine phanerogams, *P. oceanica* has a high capacity for wave attenuation as it forms extensive and dense meadows in coastal areas, with leaves that frequently exceed one meter in length Koftis et al. (2013).

The vegetation representation in the WW3 model was enhanced through the incorporation of flexibility and seasonal variability using high-resolution in-situ measurements, effectively leveraging the synergy between numerical models and observational data. The model was calibrated and validated using a rigorously measured idealized test case. These developments have led to an improved accuracy of the numerical modeling framework, which is one of the factors of the Coastal Ocean Digital Twin (Pillai et al. (2022)) along with the coupling of different components (e.g., circulation and sediments) and the ability to reproduce various scenarios.

We evaluated *PO's* ability to attenuate waves in the Civitavecchia coastal zone, where conflicts between the expansion of the Port of Civitavecchia and the sustainable management of SCIs are addressed by the RENOVATE project (Marcelli et al. (2023)). This project aims to resolve these conflicts by using a model-based approach to enhance the effectiveness of mitigation and compensation measures.

The study considered seasonal variation of plant characteristics, and three substrates which induced in *PO* different phenotypic traits. It is important to emphasize that the vegetation-induced wave damping effects analyzed here were based solely

https://doi.org/10.5194/egusphere-2025-321
Preprint. Discussion started: 3 February 2025
© Author(s) 2025. CC BY 4.0 License.

on these varying traits and not on the dissipation properties of the different substrates. Therefore, our findings offer an initial insight into the potential range of variability in vegetation-induced wave damping within a specific area, depending on the particular characteristics of the plants. Future studies will consider the different traits on various substrates, as well as the effects of vegetation seasonal variations.

The findings deliver essential guidance for local coastal management at SCIs, particularly in refining *PO* restoration strategies to strengthen coastal protection and conservation efforts. Despite these advancements, further investigation into the seasonal variations of seagrass is needed, with particular attention to abiotic factors such as irradiance, temperature, sediment characteristics, and nutrient availability, to better simulate the health status of *PO*. This approach will enable a comprehensive evaluation of how environmental conditions influence vegetation dynamics and their interaction with waves. Future research should prioritize the development of a feedback mechanism between the wave model and vegetation to facilitate restoration planning in areas with conditions conducive to seagrass growth and survival.

Appendix A

A1

Numerical propagation for the unstructured triangular grid was set to CRD-N-scheme (Ricchiuto et al. (2005)) and the spectral propagation part is solved with simple implicit 1st order upwind schemes. The linear input source term was activated for initial wave growth and consistent model spin-up, as described by Cavaleri and Rizzoli (1981), with the filter function to limit the effect of low-frequency energies at initial growth (Tolman (1992)). Sink terms due to negative wind input, whitecapping dissipation, and wave-turbulence interactions, as defined by Ardhuin et al. (2009), were also included. Nonlinear wave-wave interactions were modelled using the Discrete Interaction Approximation (DIA) (Hasselmann and Hasselmann (1985). For the bottom friction the simple linear JONSWAP parametrization derived by Hasselmann et al. (1973) was used. As a function of bottom topography, waves exceeding a threshold height, determined by a statistical description of surf-zone wave heights, were set to break and dissipate energy following the approach of Battjes and Janssen (1978). Triad nonlinear interactions were resolved using the LTA model of Eldeberky and Battjes (1996). Wind stresses were computed according to Donelan et al. (2012), while the wind field was interpolated linearly in time and space. Shoreline reflection was activated. Flexible vegetation (Eq. 4) was incorporated into the bottom friction definition, also introducing the seasonal variations where leaves grow and undergo a gradual shortening and fading process over the year as depicted in the following section. The initial leaf parameters were encoded, and a mask file was used to mark vegetation distribution and a substrate type at each location.

A2

https://doi.org/10.5194/egusphere-2025-321
Preprint. Discussion started: 3 February 2025
© Author(s) 2025. CC BY 4.0 License.

Table A1. List of symbols.

Symbol	Description	Units of measure
g	Acceleration due to gravity	LT^{-2}
U_b/UBR	Near-bed wave orbital velocity	LT^{-1}
H_s/SWH	Significant wave height	L
$\tilde{C}_D$	Drag coefficient	-
h	Water depth	L
l_v	Leaf length	L
l_e	Effective leaf length	L
b_v	Stem width	L
N_v	Vegetation (shoot) density	L^{-2}
t_v	Vegetation thickness	L
ρ_v	Tissue density	ML^{-3}
ρ	Water density	ML^{-3}
$\tilde{k}$	Average wavenumber	L^{-1}
k	Wavenumber	L^{-1}
$\tilde{\sigma}$	Average wave frequency	T^{-1}
σ	Wave frequency	T^{-1}
θ	Wave direction	-
T_{peak}	Peak wave period	T
c_g	Group velocity	LT^{-1}
U	Ambient current	LT^{-1}
$\dot{\mathbf{x}}$	Combined advection velocity	LT^{-1}
∇	Differential operator in 2-d space	L^{-1}
$\dot{\theta}$	Propagation velocity in spectral wave direction space	T^{-1}
$\dot{k}$	Propagation velocity in spectral wavenumber space	$L^{-1}T^{-1}$
S_{bot}	Dissipation term due to bottom friction	L^3T^{-2}
$S_{ds,veg}$	Dissipation term due to vegetation	L^3T^{-2}
N	Action density	L^2T^{-1}
E_{tot}	Total energy	L^2
$E(\sigma,\theta)$	Spectral energy density	L^2
E	Elastic module	$ML^{-1}T^{-2}$
Γ	Empirical constant	L^2T^{-3}
n	Ratio of phase velocity to group velocity	-
I	Second moment of area	L^4
B	The ratio of the restoring force due to buoyancy and the restoring force due to stiffness	-
Ca	Cauchy number	-
SCI	Sites of Community Importance	-

https://doi.org/10.5194/egusphere-2025-321
Preprint. Discussion started: 3 February 2025
© Author(s) 2025. CC BY 4.0 License.

Author contributions. Conceptualization: *S.S., I.F., S.B., S.C., N.P.;* Data curation: *S.S., S.B., V.P. D.P.;* Formal analysis: *S.S., S.B., S.C.;* Funding acquisition: *G.C., M.M.;* Investigation: *S.S., S.C., S.B.;* Methodology: *S.S., S.C.;* Project administration: *V.P., G.C.;* Resources: *I.F., G.C., M.M.;* Software: *S.S., S.C., N.B., J.A.;* Supervision: *I.F., N.P.;* Validation: *S.S., S.C.;* Visualization: *S.S., S.C., S.B.;* Writing – original draft: *S.S., I.F.;* Writing – review and editing: *S.S., I.F., S.C., S.B., L.M., N.P.;*

Competing interests. The authors declare that they have no conflict of interest.

Acknowledgements. This project was funded by the following projects: RENOVATE - Convenzione n. 3 Bis, Decreto 81 del 15/03/2022, Autorità di Sistema Portuale del Mar Tirreno Centro Settentrionale; FOCCUS - Project No. 101133911, EU; PNRR BIO - CN00000033, MUR; and EDITO-Model Lab - Project No. 101093293, EU.

https://doi.org/10.5194/egusphere-2025-321
Preprint. Discussion started: 3 February 2025
© Author(s) 2025. CC BY 4.0 License.

References

Abdolali, A., Hesser, T. J., Anderson Bryant, M., Roland, A., Khalid, A., Smith, J., Ferreira, C., Mehra, A., and Sikiric, M. D.: Wave Attenuation by Vegetation: Model Implementation and Validation Study, Frontiers in Built Environment, 8, https://doi.org/10.3389/fbuil.2022.891612, 2022.

Alcoverro, T., Duarte, C. M., and Romero, J.: Annual growth dynamics of Posidonia oceanica: contribution of large-scale versus local factors to seasonality, Marine Ecology Progress Series, 120, 203–210, http://www.jstor.org/stable/24851876, 1995.

Ardhuin, F., Rogers, E., Babanin, A. V., Filipot, J.-F., Magne, R., Roland, A., van der Westhuysen, A., Queffeulou, P., Lefévre, J. M., Aouf, L., and Collard, F.: Semiempirical Dissipation Source Functions for Ocean Waves. Part I: Definition, Calibration, and Validation, Journal of Physical Oceanography, 40, 1917–1941, https://api.semanticscholar.org/CorpusID:9635698, 2009.

Ardizzone, G., Belluscio, A., and Criscoli, A.: Atlante degli habitat dei fondali marini del Lazio. Regione Lazio., Direzione Regionale Capitale Naturale, Parchi e Aree Protette, 2018.

Battjes, J. A. and Janssen, J. P. F. M.: Energy Loss and Set-Up Due to Breaking of Random Waves, pp. 569–587, American Society of Civil Engineers, https://doi.org/10.1061/9780872621909.034, 1978.

Beudin, A., Kalra, T. S., Ganju, N. K., and Warner, J. C.: Development of a coupled wave-flow-vegetation interaction model, Computers & Geosciences, 100, 76–86, https://doi.org/https://doi.org/10.1016/j.cageo.2016.12.010, 2017.

Blender Community: Blender - a 3D modelling and rendering package, Blender Foundation, Blender Institute, Amsterdam, http://www.blender.org, 1994.

Bonamano, S., de Mendoza, F. P., Piermattei, V., Martellucci, R., Madonia, A., Gnisci, V., Mancini, E., Fersini, G., Burgio, C., Marcelli, M., et al.: Mathematical models supporting the monitoring of Civitavecchia harbour (Rome), WIT Transactions on Modelling and Simulation, 59, 443–454, 2015.

Bonamano, S., Piermattei, V., Madonia, A., Paladini de Mendoza, F., Pierattini, A., Martellucci, R., Stefanì, C., Zappalà, G., Caruso, G., and Marcelli, M.: The Civitavecchia Coastal Environment Monitoring System (C-CEMS): a new tool to analyze the conflicts between coastal pressures and sensitivity areas, Ocean Science, 12, 87–100, 2016.

Bonamano, S., Piazzolla, D., Scanu, S., Mancini, E., Madonia, A., Piermattei, V., and Marcelli, M.: Modelling approach for the evaluation of burial and erosion processes on Posidonia oceanica meadows, Estuarine, Coastal and Shelf Science, 254, 107 321, https://doi.org/https://doi.org/10.1016/j.ecss.2021.107321, 2021.

Bonamano, S., Aurelio Peviani, M., Burgio, C. G., Fersini, G., and Marcelli, M.: High resolution numerical modeling supporting the evaluation of the WaveSAX-2 power generation in the coastal area around the Civitavecchia port, in: EGU General Assembly Conference Abstracts, EGU General Assembly Conference Abstracts, pp. EGU–7655, https://doi.org/10.5194/egusphere-egu23-7655, 2023.

Bonamano, S., Federico, I., Causio, S., Piermattei, V., Piazzolla, D., Scanu, S., Madonia, A., Madonia, N., De Cillis, G., Jansen, E., Fersini, G., Coppini, G., and Marcelli, M.: River–coastal–ocean continuum modeling along the Lazio coast (Tyrrhenian Sea, Italy): Assessment of near river dynamics in the Tiber delta, Estuarine, Coastal and Shelf Science, 297, 108 618, https://doi.org/https://doi.org/10.1016/j.ecss.2024.108618, 2024.

Borfecchia, F., Micheli, C., Cibic, T., Pignatelli, V., Cecco, L. D., Consalvi, N., Caroppo, C., Rubino, F., Poi, E. D., Kralj, M., and Negro, P. D.: Multispectral data by the new generation of high-resolution satellite sensors for mapping phytoplankton blooms in the Mar Piccolo of Taranto (Ionian Sea, southern Italy), European Journal of Remote Sensing, 52, 400 – 418, https://api.semanticscholar.org/CorpusID:197500904, 2019.

https://doi.org/10.5194/egusphere-2025-321
Preprint. Discussion started: 3 February 2025
© Author(s) 2025. CC BY 4.0 License.

Borum, J., Duarte, C., Krause-Jensen, D., and Greve, T.: European seagrasses: an introduction to monitoring and management., p. 88, Monitoring and Managing of European Seagrasses Project, ISBN 87-89143-21-3, https://doi.org/doi.org/10.25607/OBP-1997, 2004.

Bradley, K. and Houser, C.: Relative velocity of seagrass blades: Implications for wave attenuation in low-energy environments, Journal of Geophysical Research: Earth Surface, 114, https://doi.org/https://doi.org/10.1029/2007JF000951, 2009.

Buia, M. C., Gambi, M. C., and Dappiano, M.: Seagrass systems, Biologia Marina Mediterranea, 11, 133–183, 2004.

Catucci, E. and Scardi, M.: Modeling Posidonia oceanica shoot density and rhizome primary production, Scientific Reports, 10, 16 978, 2020.

Cavaleri, L. and Rizzoli, P. M.: Wind wave prediction in shallow water: Theory and applications, Journal of Geophysical Research: Oceans, 86, 10 961–10 973, 1981.

Chen, S.-N., Sanford, L. P., Koch, E. W., Shi, F., and North, E. W.: A nearshore model to investigate the effects of seagrass bed geometry on wave attenuation and suspended sediment transport, Estuaries and Coasts, 30, 296–310, https://doi.org/10.1007/BF02700172, 2007.

Chen, W., Staneva, J., Jacob, B., Sánchez-Artús, X., and Wurpts, A.: What-if nature-based storm buffers on mitigating coastal erosion, Science of The Total Environment, 928, 172 247, https://doi.org/https://doi.org/10.1016/j.scitotenv.2024.172247, 2024.

Consortium, E. B.: EMODnet Digital Bathymetry (DTM 2016), http://doi.org/10.12770/c7b53704-999d-4721-b1a3-04ec60c87238, 2016.

Dalrymple, R. A., Kirby, J. T., and Hwang, P. A.: Wave diffraction due to areas of energy dissipation, Civil and Environmental Engineering, 110, 67–79, https://doi.org/https://ascelibrary.org/doi/10.1061/%28ASCE%290733-950X%281984%29110%3A1%2867%29, 1984.

Donelan, M. A., Curcic, M., Chen, S. S., and Magnusson, A. K.: Modeling waves and wind stress, Journal of Geophysical Research: Oceans, 117, https://doi.org/https://doi.org/10.1029/2011JC007787, 2012.

Duarte, C. M.: Temporal biomass variability and production/biomass relationships of seagrass communities., Marine ecology progress series. Oldendorf, 51, 269–276, 1989.

Dubi, A. and Tørum, A.: Wave damping by kelp vegetation, Coastal Engineering Proceedings, 1, 142–154, https://doi.org/10.9753/icce.v24.%p, 1994.

Eldeberky, Y. and Battjes, J. A.: Spectral modeling of wave breaking: Application to Boussinesq equations, Journal of Geophysical Research: Oceans, 101, 1253–1264, https://doi.org/https://doi.org/10.1029/95JC03219, 1996.

Elkalay, K., Frangoulis, C., Skliris, N., Goffart, A., Gobert, S., Lepoint, G., and Hecq, J.-H.: A model of the seasonal dynamics of biomass and production of the seagrass Posidonia oceanica in the Bay of Calvi (Northwestern Mediterranean), Ecological Modelling, 167, 1–18, https://doi.org/https://doi.org/10.1016/S0304-3800(03)00074-7, 2003.

Feagin, R., Irish, J., Möller, I., Williams, A., Colón-Rivera, R., and Mousavi, M. E.: Short communication: Engineering properties of wetland plants with application to wave attenuation, Coastal Engineering, 58, 251–255, https://doi.org/10.1016/j.coastaleng.2010.10.003, 2011.

Folkard, A. M.: Hydrodynamics of model Posidonia oceanica patches in shallow water, Limnology and Oceanography, 50, 1592–1600, https://doi.org/https://doi.org/10.4319/lo.2005.50.5.1592, 2005.

Fonseca, M. S. and Cahalan, J. A.: A preliminary evaluation of wave attenuation by four species of seagrass, Estuarine, Coastal and Shelf Science, 35, 565–576, https://doi.org/https://doi.org/10.1016/S0272-7714(05)80039-3, 1992.

Geuzaine, C. and Remacle, J.-F.: Gmsh: A 3-D finite element mesh generator with built-in pre- and post-processing facilities, International Journal for Numerical Methods in Engineering, 79, 1309–1331, https://doi.org/https://doi.org/10.1002/nme.2579, 2009.

Giraud, G.: Recensement des floraisons de Posidonia oceanica (Linne) Delile en Mediterranee., Rapports et Proces-Verbaux des Reunions-Commission Internationale pour l'Exploration Scientifique de la Mer Mediterranee (CIESM). v. 24 (4)., 1977.

https://doi.org/10.5194/egusphere-2025-321
Preprint. Discussion started: 3 February 2025
© Author(s) 2025. CC BY 4.0 License.

Giraud, G., Boudouresque, C.-F., Cinelli, F., Fresi, E., and Mazzella, L.: Observations sur l'herbier de Posidonia oceanica (L.) Delile autour de l'Ile d'Ischia (Italie), Giornale botanico italiano, 113, 261–274, https://doi.org/10.1080/11263507909426647, 1979.

Gnisci, V., de Martiis, S. C., Belmonte, A., Micheli, C., Piermattei, V., Bonamano, S., and Marcelli, M.: Assessment of the ecological structure of Posidonia oceanica (L.) Delile on the northern coast of Lazio, Italy (central Tyrrhenian, Mediterranean), Italian Botanist, 9, 1–19, 2020.

Gupta, A., Behera, M. R., and Heidarpour, A.: Numerical Modeling of Wave Damping Induced by Emerged Moving Vegetation, in: International Conference on Offshore Mechanics and Arctic Engineering, vol. 84379, p. V06AT06A013, American Society of Mechanical Engineers, https://doi.org/10.1115/OMAE2020-18588, 2020.

Hasselmann, K., Barnett, T. P., Bouws, E., Carlson, H., Cartwright, D. E., Enke, K., Ewing, J., Gienapp, A., Hasselmann, D., Kruseman, P., et al.: Measurements of wind-wave growth and swell decay during the Joint North Sea Wave Project (JONSWAP)., Ergaenzungsheft zur Deutschen Hydrographischen Zeitschrift, Reihe A, 1973.

Hasselmann, S. and Hasselmann, K. F.: Computations and Parameterizations of the Nonlinear Energy Transfer in a Gravity-Wave Spectrum. Part I: A New Method for Efficient Computations of the Exact Nonlinear Transfer Integral, Journal of Physical Oceanography, 15, 1369–1377, https://api.semanticscholar.org/CorpusID:129135885, 1985.

Infantes, E., Orfila, A., Simarro, G., Terrados, J., Luhar, M., and Nepf, H.: Effect of a seagrass (Posidonia oceanica) meadow on wave propagation, Marine Ecology Progress Series, 456, 63–72, https://doi.org/10.3354/meps09754, 2012.

Jacob, B., Dolch, T., Wurpts, A., and Staneva, J.: Evaluation of seagrass as a nature-based solution for coastal protection in the German Wadden Sea, Ocean Dynamics, 73, 699–727, https://doi.org/10.1007/s10236-023-01577-5, 2023.

Jeong, J.-S. and Lee, H. S.: Unstructured Grid-Based River–Coastal Ocean Circulation Modeling towards a Digital Twin of the Seto Inland Sea, Applied Sciences, 13, https://doi.org/10.3390/app13148143, 2023.

Koch, E. and Beer, S.: Tides, light and the distribution of Zostera marina in Long Island Sound, USA, Aquatic Botany, 53, 97–107, https://doi.org/https://doi.org/10.1016/0304-3770(95)01015-7, 1996.

Koftis, T., Prinos, P., and Stratigaki, V.: Wave damping over artificial Posidonia oceanica meadow: A large-scale experimental study, Coastal Engineering, 73, 71–83, https://doi.org/https://doi.org/10.1016/j.coastaleng.2012.10.007, 2013.

Korres, G., Oikonomou, C., Denaxa, D., and Sotiropoulou, M.: Mediterranean Sea Waves Analysis and Forecast (Copernicus Marine Service MED-Waves, MEDWAM4 system) (Version 1) [Data set]., 2023.

Lei, J. and Nepf, H.: Wave damping by flexible vegetation: Connecting individual blade dynamics to the meadow scale, Coastal Engineering, 147, 138–148, https://doi.org/https://doi.org/10.1016/j.coastaleng.2019.01.008, 2019.

Luhar, M. and Nepf, H.: Wave-induced dynamics of flexible blades, Journal of Fluids and Structures, 61, 20–41, https://doi.org/https://doi.org/10.1016/j.jfluidstructs.2015.11.007, 2016.

Luhar, M. and Nepf, H. M.: Flow-induced reconfiguration of buoyant and flexible aquatic vegetation, Limnology and Oceanography, 56, 2003–2017, https://doi.org/https://doi.org/10.4319/lo.2011.56.6.2003, 2011.

Løvås, S. M. and Tørum, A.: Effect of the kelp Laminaria hyperborea upon sand dune erosion and water particle velocities, Coastal Engineering, 44, 37–63, https://doi.org/https://doi.org/10.1016/S0378-3839(01)00021-7, 2001.

Madsen, J. D., Chambers, P. A., James, W. F., Koch, E. W., and Westlake, D. F.: The interaction between water movement, sediment dynamics and submersed macrophytes, Hydrobiologia, 444, 71–84, https://doi.org/10.1023/A:1017520800568, 2001.

Marbà, N., Díaz-Almela, E., and Duarte, C. M.: Mediterranean seagrass (Posidonia oceanica) loss between 1842 and 2009, Biological Conservation, 176, 183–190, https://doi.org/https://doi.org/10.1016/j.biocon.2014.05.024, 2014.

https://doi.org/10.5194/egusphere-2025-321
Preprint. Discussion started: 3 February 2025
© Author(s) 2025. CC BY 4.0 License.

Marcelli, M., Piermattei, V., Bonamano, S., Causio, S., Ceccherelli, G., Coppini, G., De Lucia, G. A., Del Negro, P., Falace, A., Federico, I., et al.: RENOVATE Project: ecosystem approach for compensation and mitigation actions in the coastal marine environment, in: EGU General Assembly Conference Abstracts, pp. EGU–13 554, 2023.

Mendez, F. J. and Losada, I. J.: An empirical model to estimate the propagation of random breaking and nonbreaking waves over vegetation fields, Coastal Engineering, 51, 103–118, https://doi.org/https://doi.org/10.1016/j.coastaleng.2003.11.003, 2004.

Molenaar, H., Barthélémy, D., de Reffye, P., Meinesz, A., and Mialet, I.: Modelling architecture and growth patterns of Posidonia oceanica, Aquatic Botany, 66, 85–99, https://doi.org/https://doi.org/10.1016/S0304-3770(99)00071-6, 2000.

Mork, M.: The effect of kelp in wave damping, Sarsia, 80, 323–327, https://doi.org/10.1080/00364827.1996.10413607, 1996.

OpenStreetMap contributors: Planet dump retrieved from https://planet.osm.org , https://www.openstreetmap.org, 2017.

Oprandi, A., Mucerino, L., De Leo, F., Bianchi, C., Morri, C., Azzola, A., Benelli, F., Besio, G., Ferrari, M., and Montefalcone, M.: Effects of a severe storm on seagrass meadows, Science of the Total Environment, 748, 141 373, 2020.

Ott, J. A.: Growth and Production in Posidonia Oceanica (L.) Delile, Marine Ecology, 1, 47–64, https://doi.org/https://doi.org/10.1111/j.1439-0485.1980.tb00221.x, 1980.

Owens, R. and Hewson, T.: ECMWF Forecast User Guide, Tech. rep., ECMWF, Reading, https://doi.org/10.21957/m1cs7h, 2018.

Pansini, A., Bosch-Belmar, M., Berlino, M., Sarà, G., and Ceccherelli, G.: Collating evidence on the restoration efforts of the seagrass Posidonia oceanica: current knowledge and gaps, Science of The Total Environment, 851, 158 320, https://doi.org/https://doi.org/10.1016/j.scitotenv.2022.158320, 2022.

Paul M., Bouma T.J., A. C.: Wave attenuation by submerged vegetation: combining the effect of organism traits and tidal current, Marine Ecology Progress Series, 444, 31–41, https://doi.org/10.3354/meps09489, 2012.

Pergent-Martini, C., Pergent, G., Monnier, B., Boudouresque, C.-F., Mori, C., and Valette-Sansevin, A.: Contribution of Posidonia oceanica meadows in the context of climate change mitigation in the Mediterranean Sea, Marine Environmental Research, 165, 105 236, 2021.

Piazzolla, D., Scanu, S., Mancuso, F. P., Bosch-Belmar, M., Bonamano, S., Madonia, A., Scagnoli, E., Tantillo, M. F., Russi, M., Savini, A., Fersini, G., Sarà, G., Coppini, G., Marcelli, M., and Piermattei, V.: An integrated approach for the benthic habitat mapping based on innovative surveying technologies and ecosystem functioning measurements, Scientific Reports, 14, 5888, https://doi.org/10.1038/s41598-024-56662-6, 2024.

Pillai, U. P. A., Pinardi, N., Alessandri, J., Federico, I., Causio, S., Unguendoli, S., Valentini, A., and Staneva, J.: A Digital Twin modelling framework for the assessment of seagrass Nature Based Solutions against storm surges, Science of the Total Environment, 847, https://doi.org/10.1016/j.scitotenv.2022.157603, 2022.

Remacle, J.-F., Henrotte, F., Carrier-Baudouin, T., Béchet, E., Marchandise, E., Geuzaine, C., and Mouton, T.: A frontal Delaunay quad mesh generator using the L_∞ norm, International Journal for Numerical Methods in Engineering, 94, 494–512, https://doi.org/https://doi.org/10.1002/nme.4458, 2013.

Ricchiuto, M., Csík, Á., and Deconinck, H.: Residual distribution for general time-dependent conservation laws, Journal of Computational Physics, 209, 249–289, https://api.semanticscholar.org/CorpusID:120849657, 2005.

Rifai, H., Quevedo, J. M. D., Lukman, K. M., Sondak, C. F. A., Risandi, J., Hernawan, U. E., Uchiyama, Y., Ambo-Rappe, R., and Kohsaka, R.: Potential of seagrass habitat restorations as nature-based solutions: Practical and scientific implications in Indonesia, Ambio, 52, 546–555, https://doi.org/10.1007/s13280-022-01811-2, 2023.

https://doi.org/10.5194/egusphere-2025-321
Preprint. Discussion started: 3 February 2025
© Author(s) 2025. CC BY 4.0 License.

Suzuki, T. and Dijkstra, J.: Wave propagation over strongly varying topography: cliffs and vegetation, in: 32nd Congress of IAHR, the international Association of Hydraulic Engineering & Research, Venice, Italy, edited by Prince Sultan Bin Abdulaziz, pp. 1–10, Corila, ISBN 8889405066, 2007.

Suzuki, T., Zijlema, M., Burger, B., Meijer, M. C., and Narayan, S.: Wave dissipation by vegetation with layer schematization in SWAN, Coastal Engineering, 59, 64–71, https://doi.org/https://doi.org/10.1016/j.coastaleng.2011.07.006, 2012.

Sánchez-González, J. F., Sánchez-Rojas, V., and Memos, C. D.: Wave attenuation due to Posidonia oceanica meadows, Journal of Hydraulic Research, 49, 503–514, https://doi.org/10.1080/00221686.2011.552464, 2011.

Telesca, L., Belluscio, A., Criscoli, A., Ardizzone, G., Apostolaki, E. T., Fraschetti, S., Gristina, M., Knittweis, L., Martin, C. S., Pergent, G., Alagna, A., Badalamenti, F., Garofalo, G., Gerakaris, V., Louise Pace, M., Pergent-Martini, C., and Salomidi, M.: Seagrass meadows (Posidonia oceanica) distribution and trajectories of change, Scientific Reports, 5, 12 505, https://doi.org/10.1038/srep12505, 2015.

Tolman, H. L.: Effects of numerics on the physics in a third-generation wind-wave model, Journal of physical Oceanography, 22, 1095–1111, 1992.

Unguendoli, S., Biolchi, L. G., Aguzzi, M., Pillai, U. P. A., Alessandri, J., and Valentini, A.: A modeling application of integrated nature based solutions (NBS) for coastal erosion and flooding mitigation in the Emilia-Romagna coastline (Northeast Italy), Science of The Total Environment, 867, 161 357, https://doi.org/https://doi.org/10.1016/j.scitotenv.2022.161357, 2023.

Vassallo, P., Paoli, C., Rovere, A., Montefalcone, M., Morri, C., and Bianchi, C. N.: The value of the seagrass Posidonia oceanica: A natural capital assessment, Marine Pollution Bulletin, 75, 157–167, https://doi.org/https://doi.org/10.1016/j.marpolbul.2013.07.044, 2013.

WW3DG: User manual and system documentation of WAVEWATCH III, NOAA/NWS/NCEP/MMAB, College Park, MD, USA, 2019.

Zupo, V., Buia, M., and Mazzella, L.: A Production Model forPosidonia oceanicaBased on Temperature, Estuarine, Coastal and Shelf Science, 44, 483–492, https://doi.org/https://doi.org/10.1006/ecss.1996.0137, 1997.